JOURNAL OF MATERIALS SCIENCE 20 (1985) 590–596

A transmission electron microscopic study of the Bethany iron meteorite

F. HASAN*, H. J. AXON
Department of Metallurgy and Materials Science, University of Manchester/UMIST, Manchester, UK

The Bethany iron meteorite which is a part of the Gibeon shower is a fine octahedrite with zoned plessite fields of various sizes. The optically irresolvable microstructural details inside the plessitic fields have been studied by transmission electron microscopy, and the crystallographic relationships between the primary kamacite (α) and the parent taenite (γ), and between the α and γ particles in the coarse plessite, have been examined using electron diffraction. In the case of primary kamacite the orientation-relationship with γ was close to the Nishiyama–Wasserman relationship, whereas, for the plessitic α, the orientation-relationship with γ was close to Kurdjumov–Sachs. It was also found that the $(1\,1\,1)_\gamma$ and $(1\,1\,0)_\alpha$ planes were not strictly parallel. Additionally, measurements of the composition profile through the zoned plessite have been made using STEM microanalysis technique, and related to microstructure.

1. Introduction

The Bethany meteorite forms part of the huge Gibeon shower of meteoric iron from South West Africa (Namibia) and the sample (H74.22) used in the present work was obtained from the American Meteorite Laboratory. Buchwald [1] has given a comprehensive review of the literature on this material and has described the macrostructural and optically accessible microstructural features in detail. Axon and Smith [2] made a metallographic and microprobe study of H74.22 and of samples from the British Museum (Natural History) and a preliminary study of replicas in the electron microscope have been reported by Orsini [3] and by Orsini and Cento [4].

The Gibeon meteorites, iron–nickel alloys containing 7.98% Ni; 0.44% Co; 0.02% P [1], show a macrostructure of primary "bands" of α-Fe–Ni (kamacite) which contain about 6.7% Ni and are arranged as 0.3 mm thick plates approximately parallel to the faces of an octahedron. These octahedrally oriented macroscopic "bands" of primary kamacite constitute the Widmanstätten pattern and the spaces between them are occupied by either filaments of γ-Fe–Ni (taenite; up to 40% Ni) or fields of decomposed residual γ (plessite; compositionally and structurally zoned, 28-10% Ni). The plessite fields in Gibeon are usually rimmed by structureless taenite but the nickel concentration gradient within any field, and hence the morphology of its decomposition product, depends on the size of the field.

There is no report in the literature concerning the lattice orientation-relationship between α and γ in Gibeon. However, following the early X-ray work of Young [5] on the Cañon Diablo, Butler and Carlton meteorites, it has become customary to assume a Kurdjumov–Sachs relationship in spite of the care which Young took to qualify his observations.

With the development of transmission electron microscopy and probe analysis of thin foil specimens, it has become possible to make more precise investigations of local interface crystallographic and compositional relationships and the present paper reports composition values and lattice

*Present address: Department of Metallurgy, University of Engineering and Technology, G.T. Road, Lahore-31, Pakistan.

0022–2461/85 $03.00 + .12

orientation relationships newly determined on thin foil samples. It was found possible to draw a distinction between the lattice orientation-relationship of primary kamacite with taenite and that of plessitic α with γ. Additionally, optically irresolvable details of the finer plessitic microstructures are reported and correlated with the nickel content.

2. Experimental details

Sections cut from the meteorite were metallographically polished using standard techniques and etched in 2% nital. The microstructure of these samples was optically examined and those areas which were considered to be of interest for the electron microscopic study were cut out as 3 mm diameter discs by spark-erosion technique. The discs were electrochemically thinned using a 60% ethanol–30% 2-butoxyethanol–10% perchloric acid solution, cooled to -20° C, in a Struers electropolishing apparatus operating at 40 V. These thin-foil samples were usually cleaned, before the microscopic examination, with a beam of argon ions in an Ion-Tech Super Microlap apparatus. The technique of ion-beam thinning provided a fine control on the final stages of thinning and it was possible to prepare specimens with a particular phase (or regions) of interest in the thin area.

The transmission electron microscopic examination and the STEM-microanalysis of the samples were carried out with a Philips EM400T analytical electron microscope which was equipped with an EDAX energy-dispersive X-ray detector and ancillary electronics. The weight per cent compositions were obtained from the analytical data using the ratio technique developed by Cliff and Lorimer [6]. Some chemical analyses were made on bulk samples using a Philips-505 scanning electron microscope. This microscope was also fitted with an EDAX energy-dispersive X-ray detector.

3. Results

A typical microstructure of the Bethany meteorite sample studied during the present work is shown in Fig. 1. It consists of primary "bands" of α-Fe–Ni (kamacite) and "fields" of plessite which result from the decomposition of compositionally zoned residual γ. The kamacite shows a number of thin mechanical twins which usually cross the entire width of the kamacite bands.

The microstructure within the plessite fields is shown with more detail in Fig. 2. Typically a narrow rim of taenite (γ-Fe–Ni) was present along the periphery and next to it on the inside was a dark-etching zone of irresolvable details. The microstructure at the interior of the plessitic fields consisted of a mixture of two phases, α and γ, the relative proportions of which varied with the size of the plessite field.

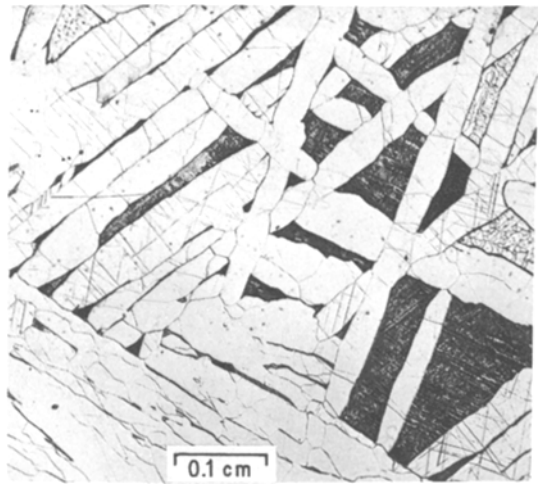

Figure 1 Widmanstätten structure in Bethany (H74.22) iron meteorite. Broad bands of kamacite (light etch) containing occasional narrow deformation twins. Ribbons and fields of plessite (variable dark etch). Optical, etched 2% nital.

The specimens for electron microscopic examination were obtained from areas similar to that shown in Fig. 2. A study of these specimens showed that the kamacite was twinned to a much greater extent than would appear from the optical

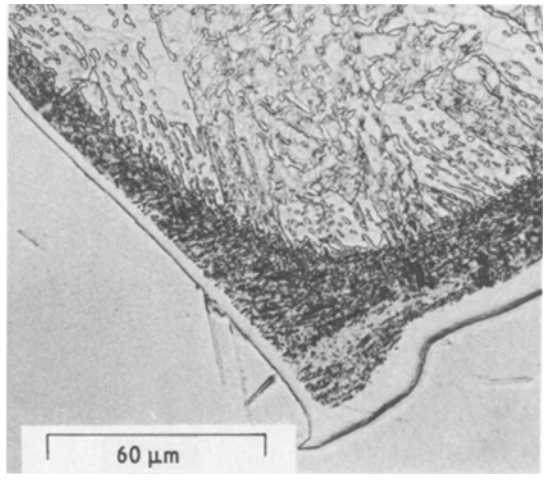

Figure 2 Enlarged detail of Fig. 1 showing a plessite field within kamacite. Note structural zones, clear taenite (γ) rim; dark martensitic zone; duplex ($\alpha+\gamma$) centre.

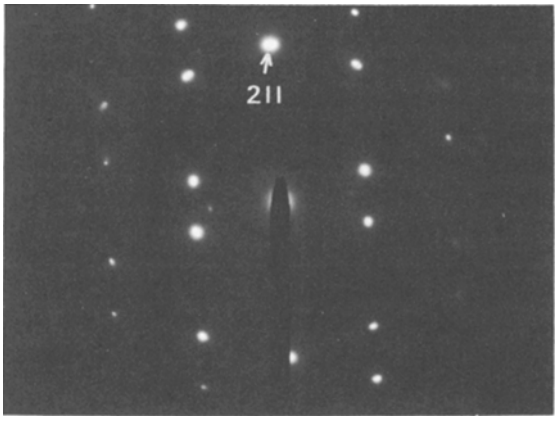

Figure 3 Electron diffraction pattern obtained from a deformation twin in the kamacite illustrating the occurrence of twinning on $\{2\,1\,1\}_{bcc}$ planes. Electron beam $\| [1\,1\,\bar{3}]_\alpha$.

microstructures. These twins were investigated by electron diffraction and were found to have formed on $\{2\,1\,1\}_{bcc}$ planes, Fig. 3.

The lattice orientation-relationship between the primary bands of kamacite and the taenite which rims the plessitic fields is illustrated by the diffraction pattern shown in Fig. 4. This orientation-relationship is neither a true Kurdjumov–Sachs (K–S) nor a true Nishiyama–Wasserman (N–W) relationship, although the deviations with respect to both are small. Nevertheless, the relationship can be regarded as being very close to an N–W orientation-relationship because: $(1\,1\,1)_\gamma \| (1\,1\,0)_\alpha$ and $[1\,\bar{1}\,0]_\gamma$ misoriented from $[0\,0\,1]_\alpha$ by $\sim 1^\circ$.

Fig. 5a shows that the dark-etching zone next to the taenite rim was martensite. The morphology of the martensite was uniform across the width of the zone; it consisted of large groups of parallel lath-shaped crystals. No α or γ particles were observed within the martensite, however, near the inside boundary of the martensitic zone small particles of γ were usually present, as shown in Fig. 5b.

At the interior of the plessite fields the decomposition to α and γ was complete and the microstructures (Figs. 6 and 2) showed small elongated particles of γ lying in rows amongst relatively larger and equi-axed grains of α. Some of these γ particles were internally twinned, Fig. 6b. The orientation-relationship between one of these γ particles and one of its neighbouring α-grains was investigated and was found to be close to the K–S relationship (Fig. 7).

Detailed electron diffraction study of the lattice orientation-relationship between primary kamacite and taenite and that between α and γ (in plessite) along such crystallographic directions that $(1\,1\,1)_\gamma$ and $(1\,1\,0)_\alpha$ planes were parallel to the electron beam revealed that there was a small misorientation between these planes. The diffraction pattern of Fig. 8, which illustrates the orientation-relationship between α and γ (plessite), was obtained with electron beam $\| [1\,1\,\bar{2}]_\gamma \| [1\,\bar{1}\,\bar{2}]_\alpha$ and shows a misorientation of $\sim 1.5^\circ$ between $(1\,1\,1)_\gamma$ and $(1\,1\,0)_\alpha$ planes.

The chemical composition of various phases and the composition profile across the zoned plessite were measured using thin-foil samples. The results presented in Fig. 9 are from a set of

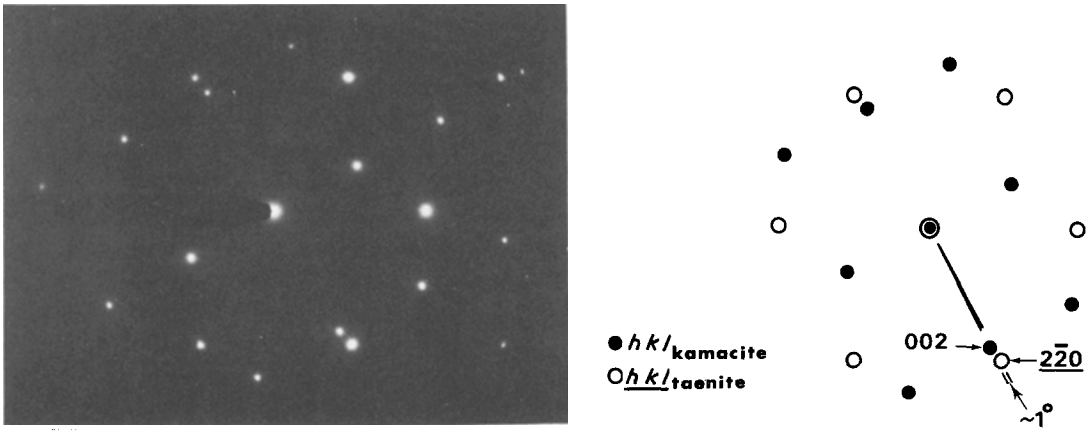

Figure 4 Electron diffraction pattern illustrating an approximately N–W lattice orientation relationship between the primary kamacite and the parent taenite. The misorientation between $[0\,0\,1]_\alpha$ and $[1\,\bar{1}\,0]_\gamma$ is $\sim 1^\circ$. Electron beam $\| [1\,1\,0]_\alpha \| [1\,1\,1]_\gamma$.

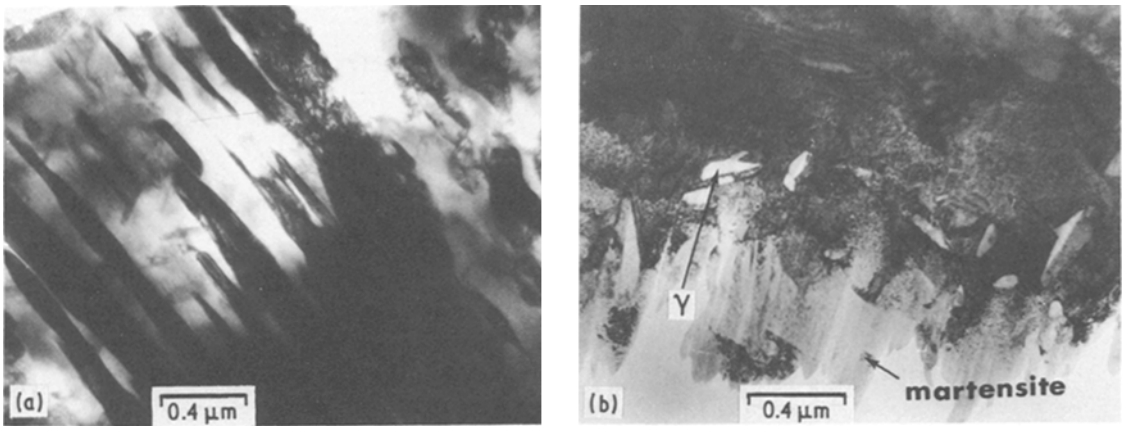

Figure 5 (a) Transmission electron micrograph showing the details of the martensitic zone in the plessite. (b) Elongated γ particles near the inside boundary of the martensite zone.

analyses carrried out along a line through kamacite–taenite (rim) – matensite–$\alpha+\gamma$ (interior). No measurable quantities of elements other than iron and nickel were detected and thus the results described in Fig. 9 are essentially the nickel contents with iron as remainder. The nickel content of the primary kamacite was quite uniform with an average value of ~6.7 %, but near the kamacite/taenite boundary it gradually decreased to about ~4.6 %, as shown in Fig. 9. On the taenite side the nickel level decreased from ~45 % (at the kamacite/taenite interface) to a value (at the interior of the plessite field) which varied with the size of the field. The composition of the martensitic zone varied from ~28 % nickel to ~20 % nickel, as shown in Fig. 9.

The average nickel-content at the interior of various plessite fields was measured in the bulk samples and the results are included in Fig. 9. The average nickel-contents varied with the size of the field, and so did the volume fraction occupied by γ; larger fields had an overall nickel content of about 9 % while smaller fields had a higher average nickel-content and a higher proportion of γ. Typical compositions of individual α and γ grains in the plessite, although their relative proportions varied, were ~6 % and ~32 % nickel, respectively. Some smaller fields had a fully martensitic structure at the interior.

4. Discussion

The fine probe size that is possible with thin foil samples allows closer investigation of interface compositions and the new values of 4.6 and 45 % Ni, respectively, for α and γ, are an improvement on the values previously [2] reported for

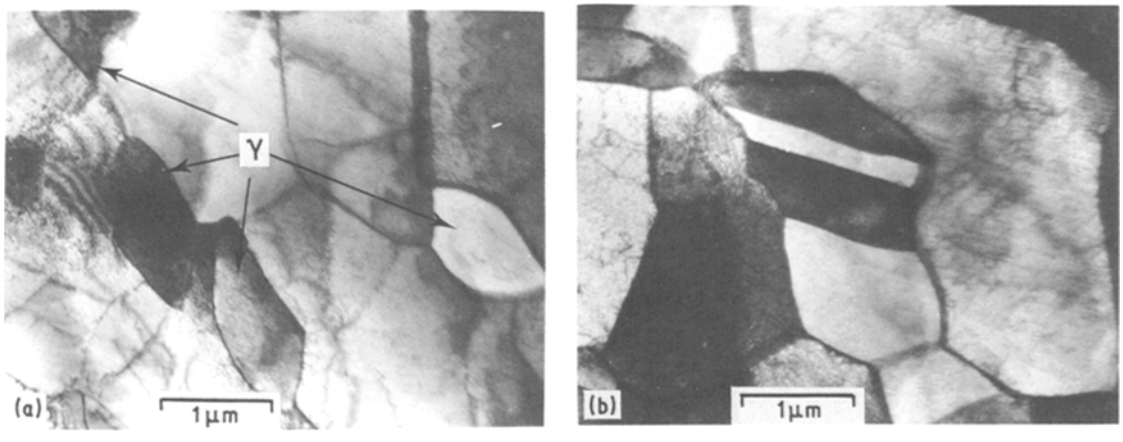

Figure 6 Transmission electron micrographs showing the structure at the interior of a plessite field: (a) elongated γ particles and equi-axed α; (b) an internally twinned γ particle.

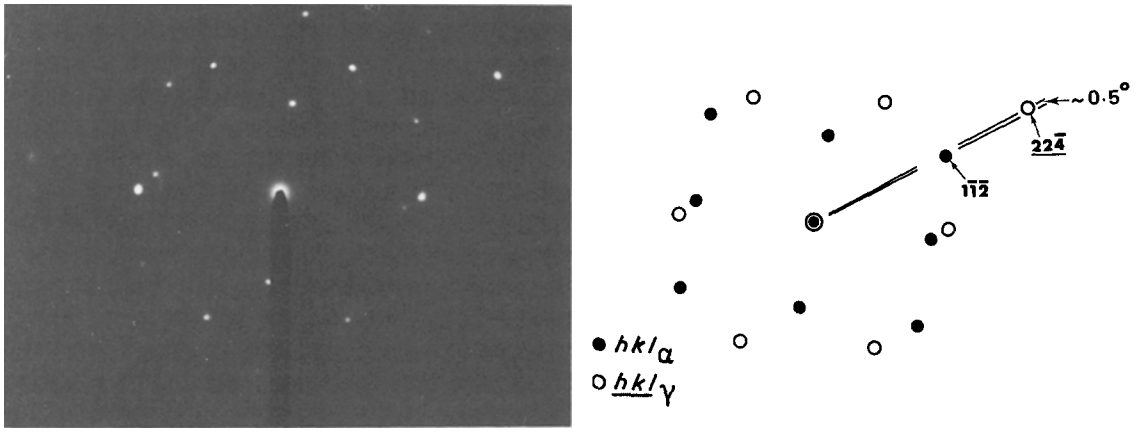

Figure 7 Electron diffraction pattern illustrating an approximately K–S orientation relationship between the α and γ in the plessite. The misorientation between $[1\,\bar{1}\,\bar{2}]_\alpha$ and $[1\,1\,\bar{2}]_\gamma$ is ~ 1/2°. Electron beam $\parallel [1\,1\,0]_\alpha \parallel [1\,1\,1]_\gamma$.

bulk samples. In addition, 32 % Ni average content of the γ particles within the coarse $(\alpha+\gamma)$ plessite is useful in providing an indication of the temperature at which the plessite may have formed. According to the binary Fe–Ni equilibrium diagram [7], γ of 32 % Ni is the equilibrium component at about 500° C. The magnitude of the Agrell depletion of nickel at the edge of the primary kamacite is greater than previously encountered [2] but the composition limits of the martensitic zones within the plessite fields are in line with previous observations on bulk samples.

Phosphide phases are absent from the structure of this material, hence the use of the binary Fe–Ni equilibrium diagram is justifiable, but it should be noted that in many other iron meteorites, phosphorus plays an important part in the nucleation and progress of transformation when the high-temperature parent alloy is cooled into the α stability range.

From their relative size and morphology it seems obvious that the bands of primary kamacite considerably predate the duplex $(\alpha+\gamma)$ structure of the coarse plessite. An effective transformation temperature of ~ 500° C was adduced for the $(\alpha+\gamma)$ plessite but the temperature at which the precipitation of primary kamacite initiated in Gibeon is less certain. With a bulk composition of 8 % Ni the binary Fe–Ni equilibrium diagram indicates a phase boundary temperature of about 710° C. Even allowing 120° C of undercooling for the precipitation of primary α from parent γ would place the start of the formation of kamacite at about 590° C. Overall, therefore, the

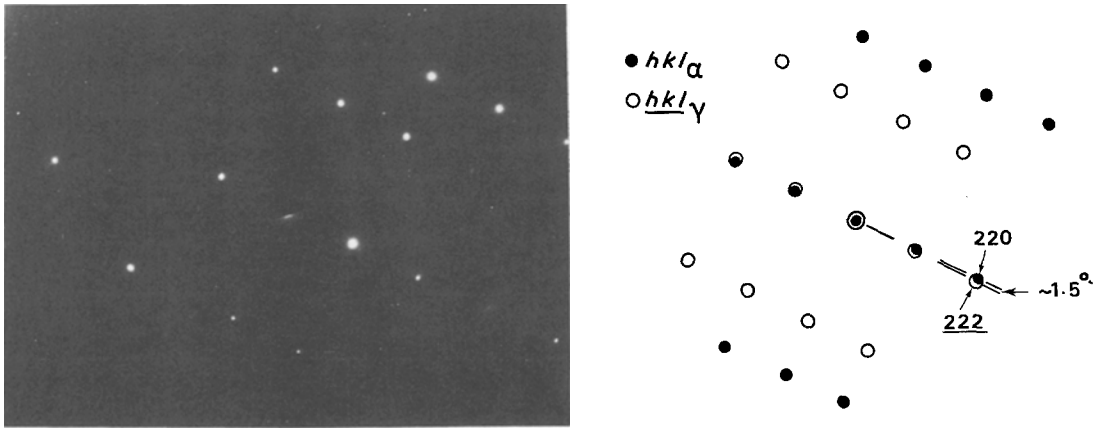

Figure 8 Electron diffraction pattern along $[1\,1\,\bar{2}]_\gamma$ and $[1\,\bar{1}\,\bar{2}]_\alpha$ zone axes illustrating the misorientation between the $(1\,1\,1)_\gamma$ and $(1\,1\,0)_\alpha$ close-packed planes.

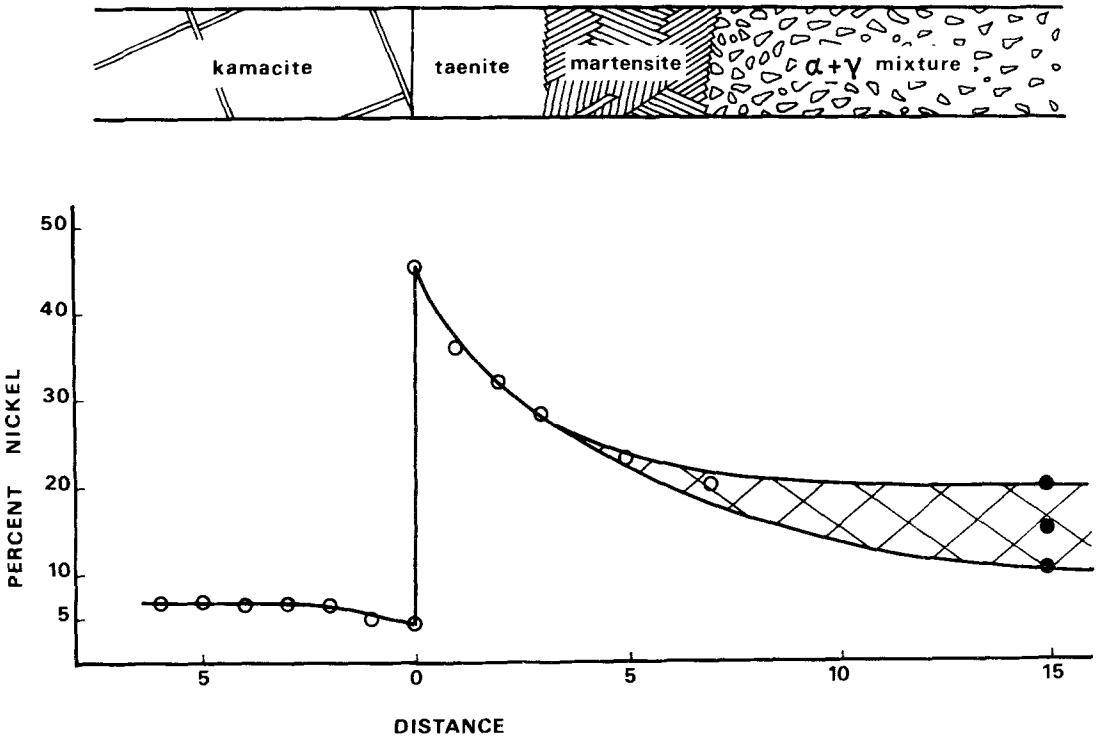

Figure 9 The composition profile across the kamacite–plessite area. Note the nickel depletion of kamacite (Agrell effect) and a nickel build-up in the taenite. (○ = thin foil analyses, • = bulk analyses.)

transformation temperatures $>600^\circ$ C and $\sim 500^\circ$ C, respectively, would appear appropriate for primary kamacite and coarse ($\alpha + \gamma$) plessite in this meteorite.

Young [5] made a detailed study of the orientation relationship between the lattices of kamacite (α) and taenite (γ) in the coarse octohedrite Cañon Diablo and reported a scatter of misorientation, with a mean value of $\sim 4^\circ$, between the $[0\,0\,1]_\alpha$ and $[1\,1\,0]_\gamma$. Additionally, he found that the close-packed planes of the two structures, i.e. $(1\,1\,0)_\alpha$ and $(1\,1\,1)_\gamma$, were not exactly parallel, the misorientation being $\sim 1.1^\circ$ (mean value). In spite of Young's emphasis on the existence of these misorientations, the relationship between the kamacite and taenite is generally regarded as K–S, i.e. $(1\,1\,1)_\gamma \| (1\,1\,0)_\alpha$; $[1\,\bar{1}\,0]_\gamma \| [1\,\bar{1}\,1]_\alpha$; $[1\,1\,\bar{2}]_\gamma \| [1\,\bar{1}\,\bar{2}]_\alpha$.

The orientation relationships determined during the present work showed similar misorientation angles between $1\,1\,0_\gamma : 0\,0\,1_\alpha$ and $1\,1\,1_\gamma : 1\,1\,0_\alpha$ as those reported by Young. From the present observations and those of Young, it is clear that the lattice orientation-relationship between kamacite (α) and taenite (γ) is neither exactly K–S nor N–W. The observation that the $(1\,1\,1)_\gamma$ and $(1\,1\,0_\alpha)$ planes are not exactly parallel, further suggests that the Widmanstätten kamacite which forms on the $(1\,1\,1)_\gamma$-octahedral planes, must have ledges at the interface to accommodate the misorientation. It is obvious that by comparison with the simple case of strictly parallel planes, a ledged interface would considerably extend the possibilities for favourable, low misfit, configurations of atoms across the α-γ interphase boundary.

The present results also showed that where the "primary kamacite:taenite" relationship was "close" to N–W (Fig. 4), the relationship between α:γ in the plessite (Fig. 7) was "close" to K–S. The difference in the two crystallographic relationships is thought to be related to the misfit energies at the interface at the respective nucleation temperatures. Thus the primary kamacite which nucleated at high temperatures exhibited an approximately N–W relationship with the parent γ, while the plessitic α which formed at relatively lower temperatures had an approximately K–S relationship with γ. Slight changes in the orientation relationship between the precipitates and the matrix have been reported to occur with changes in the

precipitate's nucleation temperatures in duplex stainless steels [8] and in nickel–aluminium bronze [9].

References

1. V. F. BUCHWALD, "Handbook of Iron Meteorites" (University of California, Berkeley 1975) pp. 584–93, 1385–93.
2. H. J. AXON and P. L. SMITH, *Mineral. Mag.* **37** (1970) 888.
3. P. G. ORSINI, *Lincei-Memoric Sc. fisiche, ecc.* 8 [section II, 3] (1967) 63.
4. P. G. ORSINI, and L. CENTO, *Ric. Sci.* **37** (1967) 725.
5. J. YOUNG, *Phil. Trans. Roy. Soc.* **A238** (1939) 393.
6. G. CLIFF and G. W. LORIMER, *J. Microscopy* **103** (1975) 203.
7. J. I. GOLDSTEIN and R. E. OGLIVIE, *Trans. Met. Soc. AIME* **233** (1965) 2083.
8. P. D. SOUTHWICK and R. W. K. HONEYCOMBE, *Met. Sci.* **14** (1980) 203.
9. F. HASAN, A. JAHANAFROOZ, G. W. LORIMER and N. RIDLEY, *Met. Trans. A* **13A** (1982) 1337.

Received 29 February
and accepted 10 April 1984